Tbx3 controls the sinoatrial node gene program and imposes pacemaker function on the atria

Willem M.H. Hoogaars,[1,3] Angela Engel,[2,3] Janynke F. Brons,[1,3] Arie O. Verkerk,[2] Frederik J. de Lange,[1] L.Y. Elaine Wong,[1] Martijn L. Bakker,[1] Danielle E. Clout,[1] Vincent Wakker,[1] Phil Barnett,[1] Jan Hindrik Ravesloot,[2] Antoon F.M. Moorman,[1] E. Etienne Verheijck,[2] and Vincent M. Christoffels[1,4]

[1]Department of Anatomy and Embryology, Academic Medical Center, University of Amsterdam, 1105 AZ Amsterdam, The Netherlands; [2]Department of Physiology, Heart Failure Research Center, Academic Medical Center, University of Amsterdam, 1105 AZ Amsterdam, The Netherlands

The sinoatrial node initiates the heartbeat and controls the rate and rhythm of contraction, thus serving as the pacemaker of the heart. Despite the crucial role of the sinoatrial node in heart function, the mechanisms that underlie its specification and formation are not known. Tbx3, a transcriptional repressor required for development of vertebrates, is expressed in the developing conduction system. Here we show that *Tbx3* expression delineates the sinoatrial node region, which runs a gene expression program that is distinct from that of the bordering atrial cells. We found lineage segregation of *Tbx3*-negative atrial and *Tbx3*-positive sinoatrial node precursor cells as soon as cardiac cells turn on the atrial gene expression program. *Tbx3* deficiency resulted in expansion of expression of the atrial gene program into the sinoatrial node domain, and partial loss of sinoatrial node-specific gene expression. Ectopic expression of *Tbx3* in mice revealed that Tbx3 represses the atrial phenotype and imposes the pacemaker phenotype on the atria. The mice displayed arrhythmias and developed functional ectopic pacemakers. These data identify a *Tbx3*-dependent pathway for the specification and formation of the sinoatrial node, and show that Tbx3 regulates the pacemaker gene expression program and phenotype.

[*Keywords*: Heart development; pacemaker; sinoatrial node; lineage; Tbx3; transgenic mice]

Supplemental material is available at http://www.genesdev.org.

Received October 26, 2006; revised version accepted March 15, 2007.

The heart rhythm of higher vertebrates is driven by pacemaker cells. In mammals, these specialized heart muscle cells reside within the sinoatrial node (SAN), a structure located in the right atrium at the junction with the superior caval vein. The SAN has a distinct phenotype compared with atria, and runs a unique ion channel and gap junction gene expression program essential for normal pacemaker function (Boyett et al. 2000; Schram et al. 2002; Marionneau et al. 2005; Liu et al. 2006). *Hcn4* encodes an isoform of the hyperpolarization-activated channels that is highly expressed in the SAN and is required for normal cardiac pacemaker activity (Baruscotti et al. 2005). Mutations in *Hcn4* result in SAN dysfunction and bradycardia in humans and mice (Schulze-Bahr et al. 2003; Stieber et al. 2003; Milanesi et al. 2006). Genes expressed in the atrial working myocardium but normally inactive in the SAN include *Nppa* (*ANF*) and *Smpx* (*Chisel*), and gap junction genes *Cx40* (*Gja5*) and *Cx43* (*Gja1*), which are essential for fast propagation of the electrical impulse in the working myocardium (Moorman and Christoffels 2003; Gros et al. 2004; Bagwe et al. 2005). Pacemaker activity is essential for heart function and viability throughout the life span of an individual. Acquired heart disease, corrected congenital heart defects, pharmacological agents, or gene defects may cause sinus node dysfunction (sick sinus syndrome), a common disorder necessitating electronic pacemaker implantation.

A century after the discovery of the SAN structure in mammals by Keith and Flack (1907), its origin and genetic control are largely unknown. Although all cardiomyocytes of the early embryonic heart display pacemaker activity, this property is lost, or suppressed, when these cells mature to working myocardial cells. However, the mature SAN still has pacemaker activity and the slow intercellular conduction also found in the embryonic cardiomyocytes, suggesting that prevention of

---

[3]**These authors contributed equally to this work.**
[4]**Corresponding author.**
E-MAIL v.m.christoffels@amc.uva.nl; FAX 31-20-6976177.
Article is online at http://www.genesdev.org/cgi/doi/10.1101/gad.416007.

differentiation of working myocardium may be an essential element of SAN formation. Recently, we found that cardiac homeobox factor Nkx2-5, which is critical for cardiogenesis and working myocardium differentiation, is absent from the sinus venosus and SAN, providing a possible mechanism for the early confinement of the pacemaker phenotype to this region (Mommersteeg et al. 2007). However, the mechanism underlying the patterning and formation of the SAN domain and the regulation of its gene program have remained unclear. Tbx3 is a T-box transcription factor uniquely expressed in the developing conduction system (Hoogaars et al. 2004). Tbx3 is a transcriptional repressor involved in developmental patterning and the regulation of proliferation, senescence bypass, and apoptosis in a variety of tissues (He et al. 1999; Brummelkamp et al. 2002; Carlson et al. 2002; Davenport et al. 2003; Naiche et al. 2005). Mutations in *TBX3* cause human ulnar-mammary syndrome, a disorder characterized by abnormal development of forelimbs, apocrine glands, teeth, and, occasionally, the heart (Bamshad et al. 1997; Meneghini et al. 2006). Because of its unique nodal expression pattern in the heart and functional equivalence to Tbx2, a potent repressor of markers for working myocardial differentiation including *Nppa*, *Smpx*, and *Cx40* in the developing heart (Habets et al. 2002; Christoffels et al. 2004b; Harrelson et al. 2004), Tbx3 is an attractive candidate regulator for the SAN gene program. Here we investigated the role of Tbx3 in the regulation of SAN formation, gene expression, and function. We found lineage segregation of differentiating atrial and *Tbx3*-positive SAN cells, indicating that the SAN is formed by proliferation of *Tbx3*-positive precursor cells, and not by recruiting adjacent myocytes that have initiated the atrial gene program. Analysis of *Tbx3*-deficient embryos revealed that Tbx3 is required to induce and maintain the SAN gene program, while preventing the expansion of atrial gene expression into the SAN domain. Ectopic *Tbx3* expression mouse models revealed that Tbx3 is sufficient to reprogram atrial cells into functional pacemaker cells that run a SAN gene program.

Results

Tbx3 defines the SAN domain

The SANs of late fetal and adult mice coexpress *Tbx3* and *Hcn4*, a key SAN marker gene (Stieber et al. 2004; Baruscotti et al. 2005), whereas *Cx40*, *Cx43*, *Smpx*, and *Nppa* are selectively expressed in the atrial myocardium in a pattern strictly complementary to that of *Tbx3* and *Hcn4* (Supplementary Fig. 1; Hoogaars et al. 2004; Mommersteeg et al. 2007). *Lbh*, encoding a putative repressor of *Nppa* (Briegel et al. 2005), was found to be expressed in the SAN and not in the atria (Supplementary Fig. 1A). Furthermore, *Hop*, encoding a transcriptional cofactor required for *Cx40* expression and function of the ventricular conduction system (Ismat et al. 2005), appeared to be expressed at relatively low levels in the SAN (Supplementary Fig. 1A). Thus, the SAN expresses *Tbx3* and runs a gene program distinct from the atrial working myocardial cells that directly border the SAN.

To assess the role of Tbx3 in the specification of SAN cells and in the regulation of gene expression, *Tbx3*-deficient mice were generated by replacing the first three codons in the first exon of *Tbx3* with a *Cre-pA* cassette (Supplementary Fig. 2). Consistent with published results (Davenport et al. 2003), homozygous mutants (*Tbx3*$^{Cre/Cre}$) died between embryonic day 11.5 (E11.5) and E14.5, displaying multiple malformations. These include limb malformations and failure to induce mammary glands, indicating that the *Cre-pA* insertion resulted in a functional null allele. Expression of *Cre* in *Tbx3*$^{Cre/Cre}$ embryos and endogenous *Tbx3* in controls was highly similar, indicating that the *Cre* expression pattern mimics *Tbx3* gene activity in mutants (Figs. 1A,D, 2D–F; Supplementary Fig. 2). To identify the primordial SAN region of interest, sections were probed for the expression of *Tbx3* in wild type and for expression of *Cre* in mutants. Morphologically, a primordial SAN was formed in *Tbx3* mutants, which expressed *Hcn4* (Fig. 1A). Quantification of the volume of the SAN in wild-type and mutant littermates revealed that it was variable in size, but on average significantly smaller in mutants (Fig. 1C). Histological analysis of E12.5 and E14.5 SANs and three-dimensional (3D) reconstruction of an E14.5 SAN revealed that the wild-type and mutant SAN had comparable length along the right sinus horn, but differed in thickness (Fig. 2A,B,D,F). We next assessed the expression of *Cx43*, *Cx40*, *Nppa*, and *Smpx*, which in the embryonic heart mark differentiating atrial and ventricular working myocardium (Christoffels et al. 2004a). Throughout development, expression of these markers was excluded from *Tbx3*-positive myocardium of wild-type embryos. At E12.5, the expression domains of *Cx43* and *Smpx* protruded into the *Cre*-positive primordial SAN of mutants (Fig. 1A,B,D). *Cx40* and *Nppa* were not ectopically expressed in the SAN at this stage, probably because Nkx2-5, a crucial activator of these genes, is not yet expressed in the sinus venosus and SAN (Mommersteeg et al. 2007). However, from E13.5 onward, also *Cx40* and *Nppa* were ectopically expressed in the SAN domain (Fig. 2B–E). 3D reconstruction and quantification and of *Tbx3*/*Cre* and *Cx40* expression domains revealed that at E14.5, almost half of the mutant SAN coexpressed *Cre* and *Cx40*, whereas *Cx40* was excluded from the SAN domain of wild-type littermates. In the region of *Cre-Cx40* coexpression, *Cx40* expression spanned the entire SAN domain from the atrium to the endothelial lining of the sinus horn (Fig. 2D). The cardiac sodium channel Na$_v$1.5 (Scn5a), which in adults is expressed in working myocardium but at much lower levels in the SAN, is essential for impulse propagation (Papadatos et al. 2002; Lei et al. 2004). We observed that also at embryonic stages, Na$_v$1.5 was almost undetectable in the developing SAN. However, a striking induction of expression was observed in the SAN domain of *Tbx3* mutants (Fig. 1E). In *Tbx3* mutants, *Lbh* expression was down-regulated in the SAN (Fig. 2F), indicating that

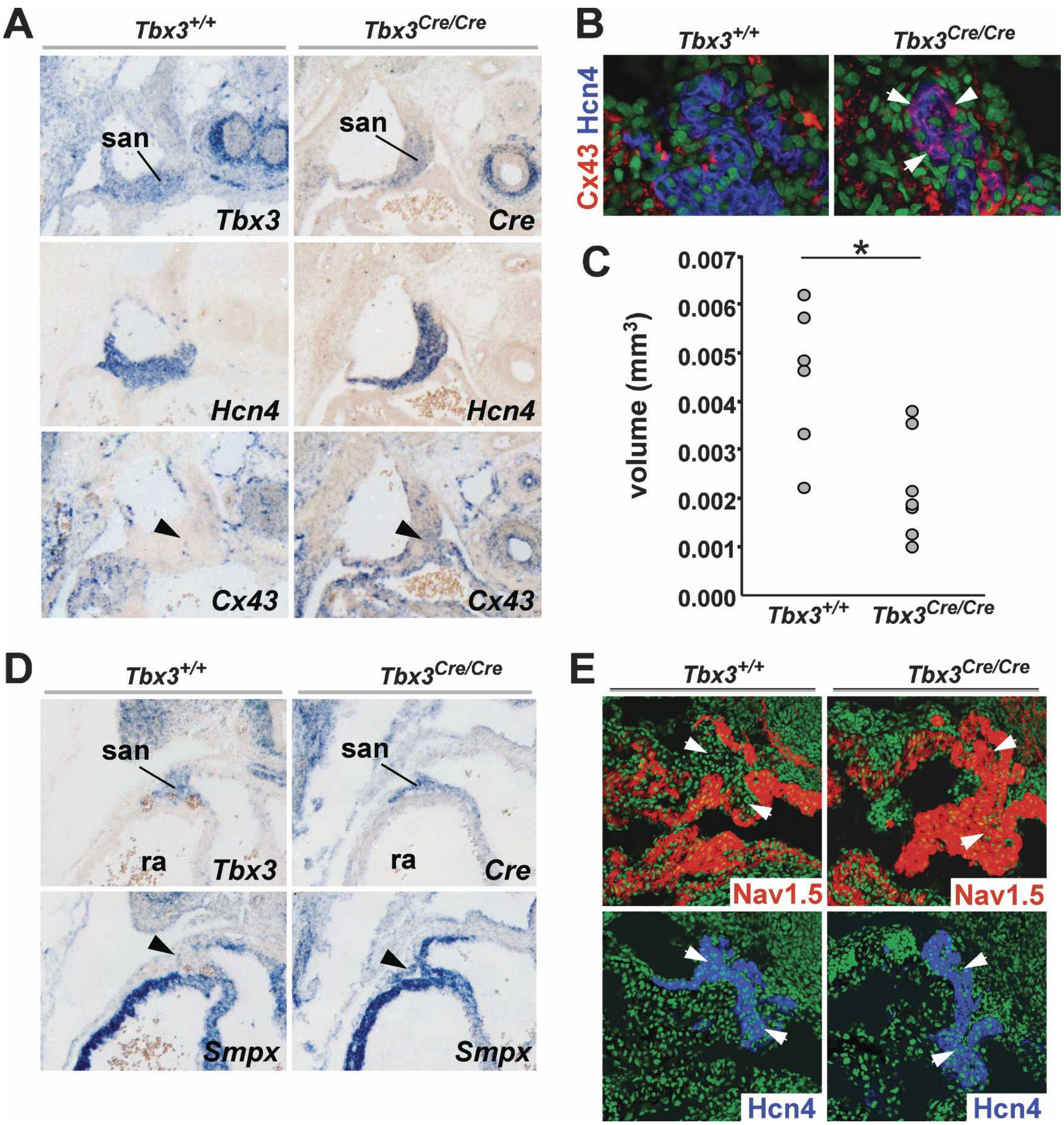

Figure 1. Tbx3 is required to suppress atrial genes in the SAN domain. (*A*) Ectopic expression of *Cx43* in the *Cre*-positive SAN of a *Tbx3*-deficient ($Tbx3^{Cre/Cre}$) embryo at E11.5 (black arrowheads). No difference in *Hcn4* expression was observed between $Tbx3^{+/+}$ and $Tbx3^{Cre/Cre}$ embryos. (*B*) Immunofluorescent double labeling of Cx43 (red) and Hcn4 (blue), and sytox green nuclear staining (green). In $Tbx3^{Cre/Cre}$ embryos, Cx43 showed overlap of expression (purple) with Hcn4 in the SAN region (white arrowheads). (*C*) Quantification of the volume of the SAN region (Tbx3 or Cre SAN expression domain) of individual E12.5 $Tbx3^{+/+}$ and $Tbx3^{Cre/Cre}$ embryos (gray dots). The average SAN volume was significantly smaller in mutants; (*) $P < 0.05$. (*D*) Expression of *Smpx* in an E11.5 $Tbx3^{+/+}$ embryo and $Tbx3^{Cre/Cre}$ littermate, showing ectopic expression in the developing SAN of $Tbx3^{Cre/Cre}$ embryos (black arrowheads). (*E*) Immunofluorescent labeling of Nav1.5 (red, *top* panel) and Hcn4 (blue, *bottom* panel) reveals ectopic expression of Nav1.5 in the Hcn4-positive SAN region of $Tbx3^{Cre/Cre}$ embryos (white arrowheads).

Tbx3 not only suppresses atrial genes, but in some cases is also required for gene activity in the SAN. We did not observe abnormalities in gene expression in heterozygous $Tbx3^{+/Cre}$ embryos and adults. These observations demonstrate that a low dose of Tbx3 is required and sufficient to suppress atrial genes in the SAN domain and to activate *Lbh*.

Differentiating atrial cells do not contribute to the Tbx3-positive SAN domain

Central conduction system components have been proposed to grow by continuous recruitment of cardiomyocytes into an initial framework of specified conduction system cells (Cheng et al. 1999; Pennisi et al. 2002). This

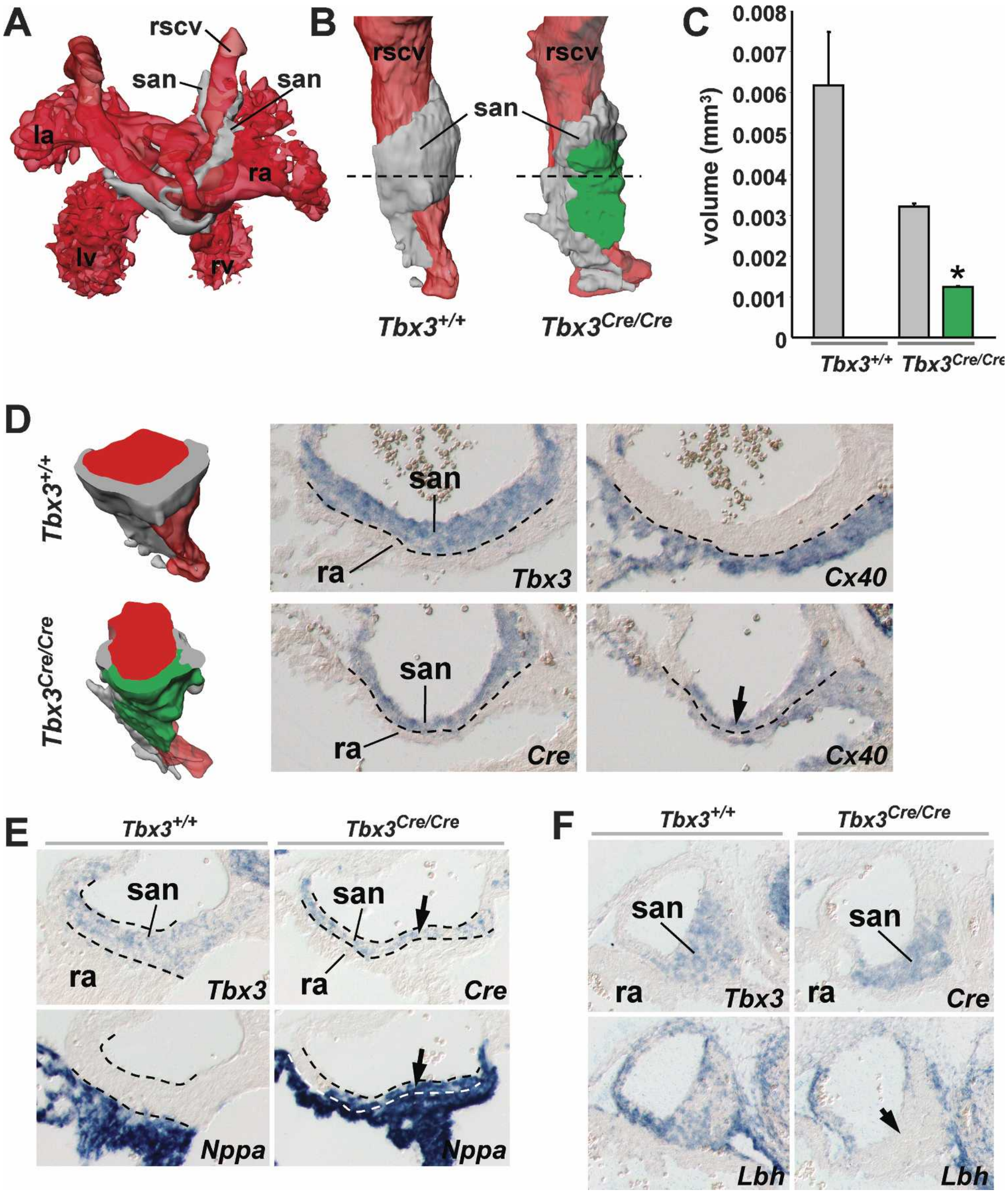

Figure 2. 3D reconstruction and expression analysis of the SAN region of *Tbx3*$^{+/+}$ embryos and *Tbx3*$^{Cre/Cre}$ embryos. (*A*) Dorsal view of a 3D reconstructed E14.5 heart. The myocardium has been removed, exposing the blood-filled lumen (red). The Tbx3-expressing myocardial is shown in gray. The SAN region is embedded between the right atrium (ra) and right superior caval vein (rscv). (*B*) 3D reconstruction of serial sections of the SAN region in *Tbx3*$^{+/+}$ embryos and *Tbx3*$^{Cre/Cre}$ embryos showing the *Tbx3*/*Cre*-positive SAN region (gray) and the lumen of the rscv (red). The atrium has been removed. *Cx40* expression in the SAN domain (Cre+) is shown in green. The dashed line depicts cross-sections through the reconstructions shown in *D*. (*C*) Average of the volume of the SAN regions (gray) and *Cx40*-positive SAN regions (green) of E14.5 *Tbx3*$^{+/+}$ embryos (n = 4) and *Tbx3*$^{Cre/Cre}$ embryos (n = 3). Error bars show the SD. Only in *Tbx3*$^{Cre/Cre}$ embryos was *Cx40* expressed in the SAN region; (*) $P < 0.05$. (*D*) *Left* panels show cross-sections of 3D reconstructions shown in *B* (dashed lines). The *right* panels show the sections at that level. Dashed lines depict border between the SAN (Tbx3+/Cre+) and the atrium. Note that *Cx40* is expressed throughout the SAN region in the *Tbx3*$^{Cre/Cre}$ embryo (black arrow). (*E*) Ectopic expression of *Nppa* in the SAN of an E14.5 *Tbx3*$^{Cre/Cre}$ embryo. Black arrow depicts *Nppa* expression in the *Cre*-positive SAN region. (*F*) Absence of *Lbh* expression in the *Cre*-positive SAN of an E13.5 *Tbx3*$^{Cre/Cre}$ embryo.

implies that the *Tbx3*-positive SAN precursor pool is continuously supplemented with adjacent myocardial cells that adopt the SAN gene program. Alternatively, the SAN may form by proliferation of conduction system precursor cells specified early in development (Fig. 3A,B). From approximately E9.5 onward, the expression of *Tbx3* allows the identification of the putative specified SAN precursors, whereas *Nppa* and *Cx40* identify the bordering atrial cells differentiating from E9.5 onward (Christoffels et al. 2000; Hoogaars et al. 2004). To assess whether these atrial cells are being recruited into the *Tbx3*-positive SAN precursor pool after their differentia-

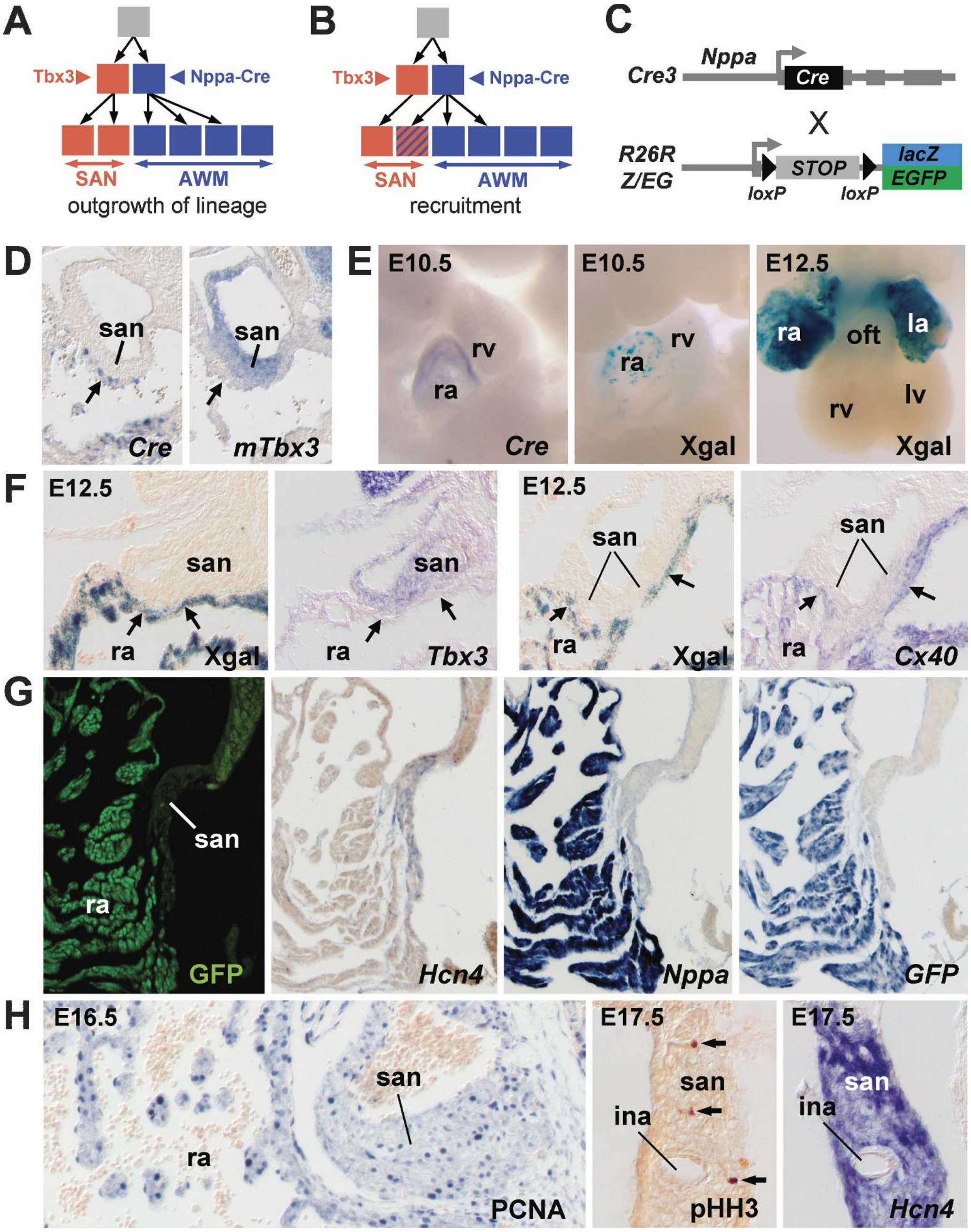

Figure 3. Early specification of SAN precursor pool: Growth of the SAN does not occur by recruitment of atrial cells. (*A*,*B*) Schemes showing two mechanisms of SAN specification: growth of a pool of specified SAN precursors (*A*) or recruitment of myocardial cells into the SAN lineage (*B*). (*C*) Transgenes used to trace the fate of myocytes after they initiated the atrial gene expression program. A cross of *Cre3* mice with *R26R* or *Z/EG* reporter mice results in activation of the *lacZ* or *EGFP* gene, respectively, in atrial myocardium. (*D*) Restricted expression of *Cre* in atrial working myocardium but not in *Tbx3*-positive SAN myocardium. (*E*) *Cre* is expressed in atrial myocardium from E10.5, as shown in whole-mount in situ hybridization and X-gal staining of *Cre-R26R* embryos. At E12.5, robust Cre-mediated recombination is observed in atrial myocardium. (*F*) Serial sections showing *Cre*-mediated *lacZ* activation in *Cx40*-positive atrial myocardium but not in the *Tbx3*-positive SAN region of E12.5 hearts. (*G*) Cross of *Nppa-Cre* mice with a *Z/EG* reporter mouse line resulting in expression of EGFP in atrial myocardium. Analysis of serial sections of adult *Cre3-Z/EG* mice revealed that EGFP expression is restricted to *Nppa*-positive atrial myocardium. The *Hcn4*-positive SAN region remained free of cells derived from EGFP-positive cells. (*H*) Presence of proliferating cells in the SANs of E16.5 and E17.5 hearts as demonstrated by the presence of PCNA and phosphorylated histone H3 (pHH3) in the *Hcn4*-positive SAN region. Black arrows show pHH3-posive cells in the SAN. (ina) Internodal artery.

tion, we deployed mice carrying an allele that expresses *Cre* under control of *Nppa* regulatory sequences (*Cre3*) (de Lange et al. 2003) selectively in the emerging atrial cells and not in the *Tbx3*-positive SAN domain (Fig. 3D). *Cre3* mice were crossed with either *R26R* or *Z/EG* reporter mice to permanently label *Cre*-expressing cells and their daughters in double transgenic offspring (Fig. 3C). From their differentiation onward, atrial cells expressed *Cre*, resulting in β-galactosidase activity from the recombined *lacZ* gene from E10.5 onward (Fig. 3E). The expression domains of *Cx40* and of *Cre3*-activated β-galactosidase activity colocalized, whereas β-galactosidase activity was not observed in the *Tbx3*-positive domain (Fig. 3F). We then investigated the expression borders in adults. Enhanced green fluorescent protein (*EGFP*) expression activated by *Cre3* exactly matched *Nppa* expression, and *Hcn4* expression was strictly complementary (Fig. 3G). We conclude that from approximately E10 on, the cells that differentiate to atrial myocardium (i.e., *Cx40*/*Nppa*-positive) and their daughters do not contribute to the SAN (i.e., *Hcn4*/*Tbx3*-positive), which therefore must increase in size by proliferation. Consistently, PCNA and phospho-histone H3 detection indicated that proliferation occurs at least until shortly before birth (Fig. 3H).

Atria of Cre-CT mice switch to the SAN gene program

Because Tbx3 is partially redundant and mutants are embryonic lethal, *Tbx3*-deficient embryos do not allow detailed assessment of the function of *Tbx3* in the regulation of the SAN phenotype. Therefore, to further explore the role of Tbx3 in regulating the SAN gene program and phenotype, we used a gain-of-function approach. Mice were generated that allow conditional activation of the human *TBX3* cDNA by Cre recombinase (*CT* mice). In these mice, Cre-mediated excision of the *CAT* reporter gene activates *TBX3* (Fig. 4A,D). *CT* mice were crossed with *Cre3* mice in order to effectively expand the SAN *Tbx3* expression domain into the atria. In double transgenic fetuses, *TBX3* was induced in the atria, whereas *Nppa* promoter-driven *Cre* expression had disappeared (Fig. 4B–D; Supplementary Fig. 3A), showing that Tbx3 in vivo suppresses the *Nppa* promoter fragment that

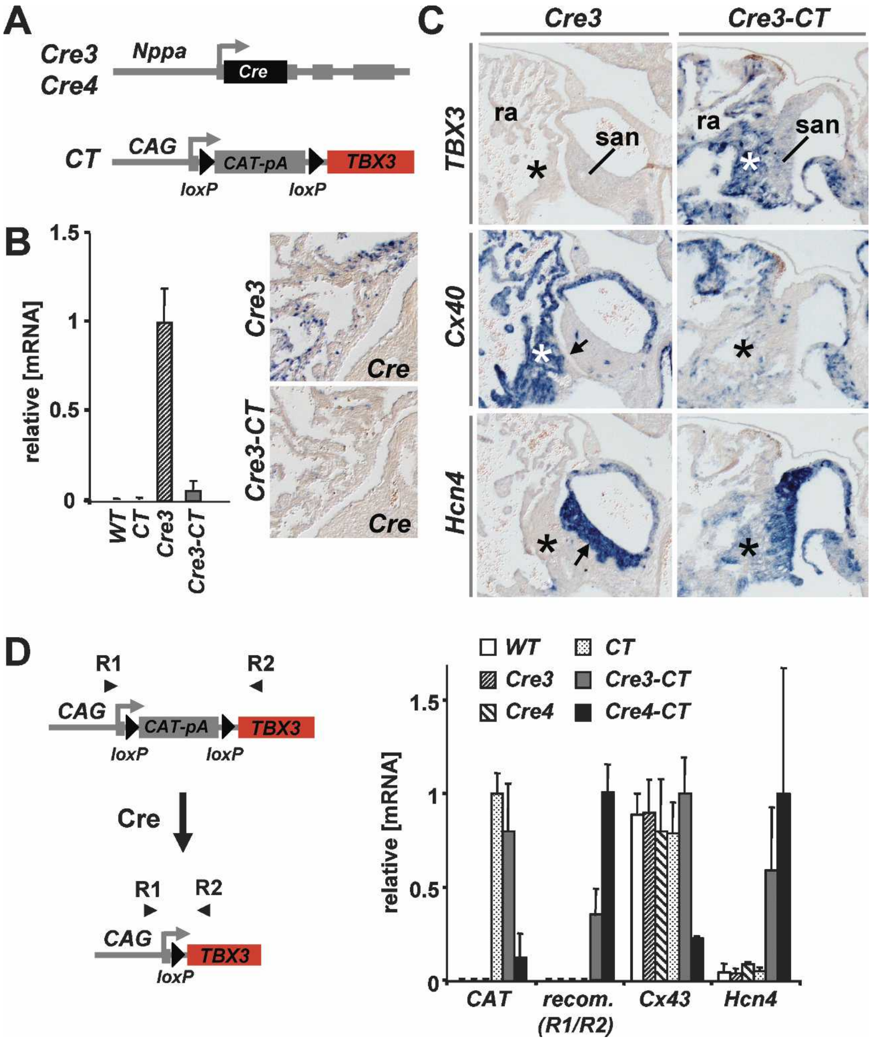

Figure 4. Ectopic expression of *TBX3* in atrial cardiomyocytes results in repression of *Cx40* and in ectopic activation of pacemaker channel *Hcn4*. (*A*) Scheme showing the *CT* and *Cre3*/*Cre4* alleles. (*B*) QRT–PCR and in situ hybridization analysis of *Cre3* mice and *Cre3-CT* double transgenic mice. *Cre* expression under control of *Nppa* regulatory sequences is repressed in *Cre3-CT* mice, demonstrating that TBX3 is capable of suppressing *Nppa* promoter activity in vivo. (*C*) In situ hybridization on serial sections of prenatal (E17.5) *Cre3* and *Cre3-CT* hearts showing *TBX3* expression, down-regulation of *Cx40*, and ectopic induction of *Hcn4* in the right atrium (ra) of *Cre3-CT* mice. Asterisks (*) depict comparable regions in the right atrium adjacent to the SAN. (*D*) QRT–PCR analysis of atria of *Cre3-CT* and *Cre4-CT* double transgenic mice compared with control mice. Expression of *Cx43* is significantly down-regulated in *Cre4-CT* mice. Due to the partial, mosaic activation of *TBX3* by *Cre3*, many atrial cells are not affected, and the repression of *Cx43* is not observed in homogenates of *Cre3-CT* mice. Expression of *Hcn4* is significantly up-regulated in both *Cre3-CT* and *Cre4-CT* mice. The product obtained with primer set R1/R2 reveals the activated TBX3-encoding transcripts.

drives *Cre* expression. Furthermore, *Cx40* and *Nppa* expression was down-regulated, whereas *Hcn4* expression was strikingly induced in these atria (Fig. 4C; data not shown). These results indicate that Tbx3 is able to repress atrial genes and to induce a SAN gene in differentiated (*Nppa*-positive) atrial cardiomyocytes. Taken together, our data indicate that Tbx3 defines a domain where atrial working myocardial genes are repressed and expression of SAN-specific genes is permitted or induced, thereby establishing a phenotypic boundary between the SAN domain and the atrial working myocardium.

We next crossed *CT* mice to *Nppa-Cre4* (*Cre4*) mice, because *Cre3*, while efficiently recombining *R26R* or *Z/EG* alleles, appeared to recombine and activate the *CT* allele less efficiently and in a mosaic pattern (Fig. 4D; Supplementary Fig. 3). Hence, while on sections effective down-regulation of target genes could be assessed in a fraction of the atrial cells, this was not possible by quantitative RT–PCR (QRT–PCR) analysis due to the large fraction of cells in which *TBX3* was not activated (Fig. 4D; Supplementary Fig. 3A,B). In contrast, the efficient activation of *TBX3* by *Cre4* allowed the assessment of gene repression by QRT-PCR (Fig. 4D). Three sets of genes were selected for expression analysis in the left atria of adult *Cre4-CT* mice. Set 1 genes represent cardiac transcription factors and structural and functional genes not enriched in either the SAN or atria (Schram et al. 2002; Marionneau et al. 2005). Set 2 genes are expressed at higher levels in the working myocardium of the atria, compared with the SAN, and are important for working myocardial function (Supplementary Fig. 1; Schram et al. 2002; Marionneau et al. 2005). This set includes *Kir2.1* and *Kir2.2,* which encode inward rectifier potassium currents involved in the fast terminal repolarization and maintenance of the resting membrane potential of working cardiomyocytes (Miake et al. 2002). Set 3 genes are expressed at higher levels in the SAN compared with the atria, and are important for SAN function (Supplementary Fig. 1; Schram et al. 2002; Marionneau et al. 2005; Liu et al. 2006). This set includes the Hcn family of hyperpolarization-activated channels, which provide pacemaker activity (diastolic depolarization) to the myocardium (Baruscotti et al. 2005). Although *Hcn4* is the dominant isoform in the SAN, *Hcn1* and *Hcn2* are also expressed in the SAN, at higher levels than in the atria (Marionneau et al. 2005). *Cav3.1* encodes a T-type calcium channel that contributes to SAN pacemaker activity (Mangoni et al. 2006). *Cx30.2* encodes a gap junction protein selectively expressed in the SAN and atrioventricular node of the conduction system that slows conduction velocity within the node (Kreuzberg et al. 2006). In situ hybridization of late fetal hearts, immunofluorescent labeling of adult hearts, and QRT–PCR analysis of adult atria showed that the genes required for regulation and function of cardiomyocytes in general, the set 1 genes, were not affected by *TBX3* expression in the atria of *Cre4-CT* mice (Figs. 5B 6A). In contrast, all atrial tissue-enriched genes were significantly down-regulated, indicating that atrial myocytes adopt low levels of expression of these genes similar to the SAN (Figs. 5A,B, 6A). The SAN-enriched genes were up-regulated in the left atria of *Cre4-CT* mice (Figs. 5A,B, 6B), especially *Hcn4* and *Cx30.2*. These data further indicate that *Tbx3* converts the atrial gene program to the SAN gene program by coordinately activating and repressing key components of each program (Fig. 6C).

To assess changes in target gene expression in response to a short period of Tbx3 exposure, α*Mhc-Cre* mice were crossed to *CT* mice in order to activate *TBX3* in the heart of embryos prior to and during chamber differentiation (Fig. 7A). Differentiation and expansion of the chamber myocardium were mildly to severely impaired (data not shown). *Cx40* and other genes specific for the atrial and ventricular chambers were efficiently down-regulated in both mildly and severely affected hearts, indicative for a relative fast response to Tbx3 exposure (1–2 d) (Fig. 7A,B). In contrast, *Hcn4*, *Cx30.2*, and *Lbh* were not induced, which indicates that up-regulation of these genes, as observed in *Cre3/4-CT* mice, is indirect, requiring prolonged presence of Tbx3 (Fig. 7B).

Both promoters of *Nppa* and *Cx43* contain a T-box-binding element (TBE) required for their suppression in the atrioventricular canal and limb in vivo, respectively (Habets et al. 2002; Chen et al. 2004), indicating that Tbx3 directly represses these genes. To assess whether Tbx3 interacts with the *Cx43* gene in vivo, chromatin was isolated from H10 rat cardiomyocyte cells (Jahn et al. 1996) stably expressing Flag-tagged Tbx3. Figure 7C shows the immunoprecipitation of chromatin using anti-Flag Sepharose with subsequent PCR amplification for the *Cx43* promoter TBE (Chen et al. 2004). Only in the presence of Tbx3 can the TBE be amplified. These results indicate that *Cx43* is directly repressed by Tbx3.

Tbx3 induces the formation of ectopic pacemaker sites in the atria

Next, we investigated whether the switch to the SAN gene program in atria of double transgenic mice was sufficient to generate functional pacemaker activity. *Cre4-CT* mice developed dilatation and fibrosis of the atria several weeks after birth, possibly resulting from electrical and structural remodeling (Supplementary Fig. 4A,B). Therefore, we used *Cre3* mice that provide an incomplete, mosaic *TBX3* activation pattern of the *CT* allele in the atria (Fig. 4; Supplementary Fig. 3). As expected, the response of Tbx3 target genes in the atria of *Cre3-CT* was comparable with that in atria of *Cre4-CT* mice, but less pronounced (Supplementary Fig. 4C,D). Whole-mount and histological examination of adult atria of *Cre3-CT* mice and controls revealed no abnormalities in size or tissue structure (Supplementary Fig. 4A,B). Electrocardiography revealed normal RR, PQ, QRS, and QT intervals and individual waveforms in the double transgenic mice (Fig. 8A,B). However, close examination of the RR intervals of double transgenic mice showed periods of normal activity ranging from seconds to minutes followed by short periods of one to three irregular, premature beats (Fig. 8A,C).

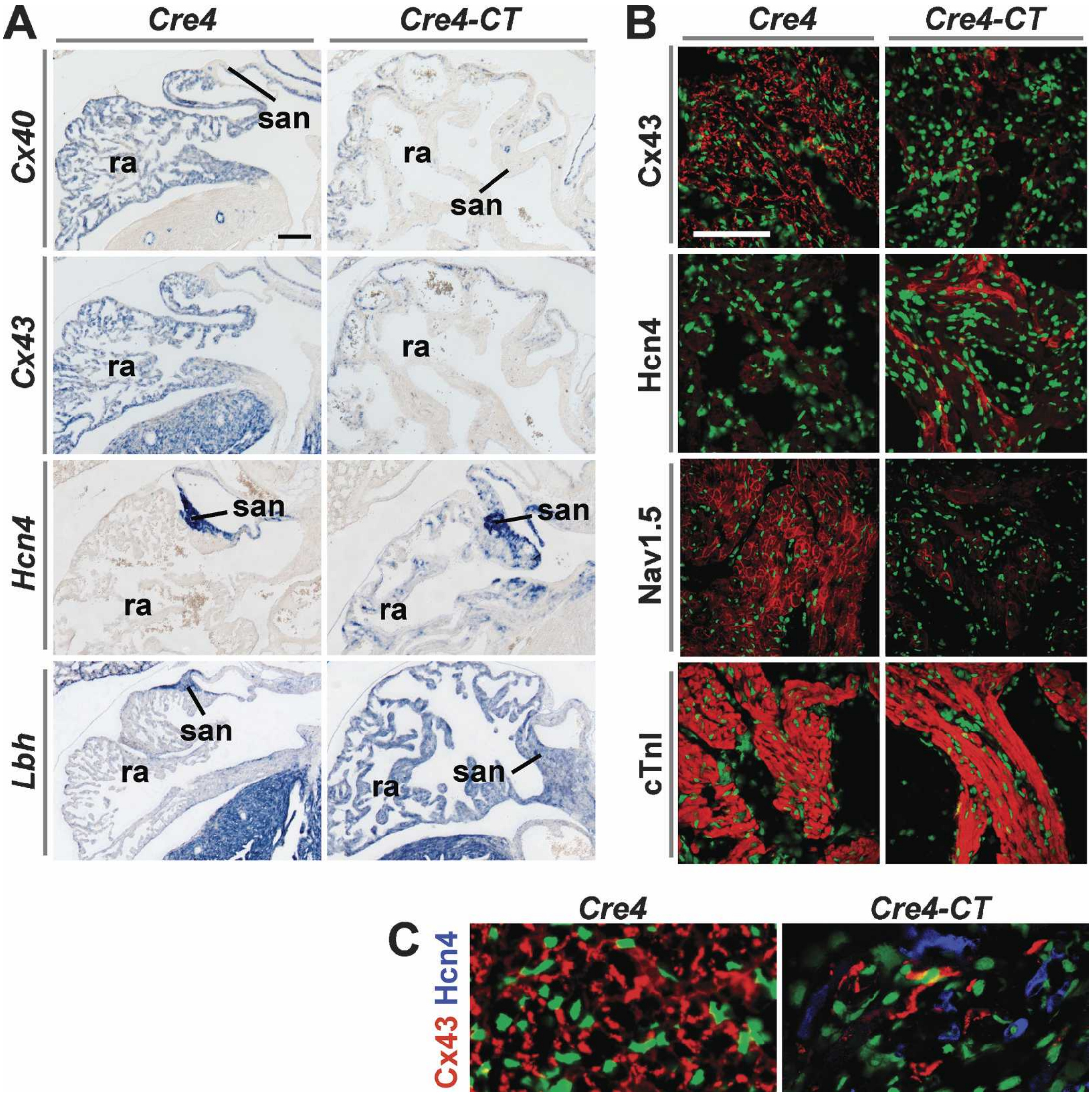

Figure 5. TBX3 represses atrial working myocardial genes and induces SAN-specific genes. (*A*) In situ hybridization of serial sections of E17.5 hearts, showing down-regulation of *Cx40* and *Cx43* in the right atrium (ra) of *Cre4-CT* mice. Expression of *Hcn4* and *Lbh* is up-regulated in atrial myocardium of *Cre4-CT* mice. (*B*) Immunofluorescent labeling of postnatal mouse heart sections showing that atrial myocytes of adult *Cre4-CT* mice ectopically expressed Hcn4, whereas Cx43 and Nav1.5 expression was reduced compared with control mice. (*C*) Immunofluorescent double staining of Cx43 (red) and Hcn4 (blue) in right atrial sections of *Cre4* and *Cre4-CT* mice, respectively. In *Cre4-CT* mice, Cx43 is down-regulated, and the residual Cx43 expression is complementary to ectopic Hcn4 expression. Bar, 100 µm.

The arrhythmia in *Cre3-CT* mice could result from dysfunction of the SAN, due to an increase in atrial premature complexes, or ectopic pacemaker activity. To discriminate between these possibilities, intact left and right atria of *Cre3-CT* mice were isolated free from SAN and internodal tract myocytes (Fig. 8D; Yamamoto et al. 2006). Ninety percent of right and 40% of left atria, respectively, showed ectopic spontaneous electrical activity, while this was absent in control mice (Fig. 8D). Mapping of the activation pattern of isolated atria in double transgenic mice revealed at least one stable ectopic pacemaker. Nodal-like action potentials could be recorded at the site of the earliest activation in the ectopic pacemaker region (Fig. 8E). To exclude cell-to-cell coupling-induced modifications, pacemaker activity was studied in isolated right atrial myocytes. Pacemaker formation was observed in seven out of 15 single myocytes (47%) of *Cre4-CT* mice, while it was absent from single myocytes (n = 11) of control mice (P = 0.01) (Fig. 8F). The spontaneously active *Cre4-CT* myocytes had nodal-like action potentials with typical low action potential upstrokes, maximal diastolic depolarization potential around −60 mV, and diastolic depolarization resulting in pacemaker activity with an intrinsic cycle length of 243 ± 61 msec. The myocytes of *Cre4-CT* mice exhibiting pacemaker activity had a clear hyperpolarization activated current

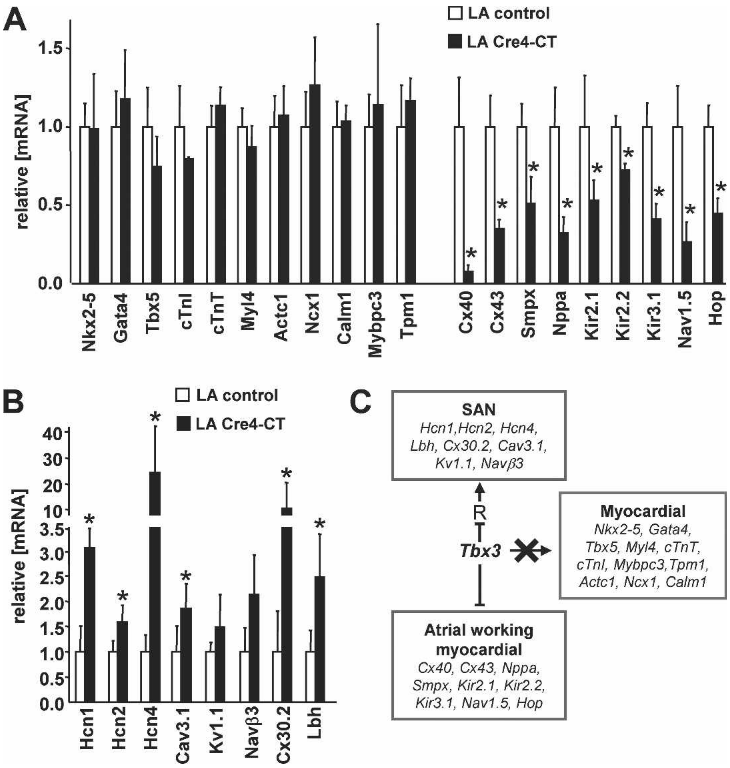

Figure 6. TBX3 induces switch to the SAN gene expression program in the atria. (*A*, *left* panel) QRT–PCR analysis showed no difference in expression of set 1 (myocardial) genes in the left atria (LA) of *Cre4-CT* mice (black bars) as compared with control mice (white bars). (*Right* panel) Expression levels of set 2 (atrium-enriched) genes showed a significant down-regulation. (*B*) Expression levels of set 3 (SAN-enriched) genes were induced in the *left* atria of *Cre4-CT* mice. (*C*) Scheme indicating a central role for Tbx3 in the regulation of the SAN gene program and phenotype. Because Tbx3 is a repressor, it may activate genes indirectly (i.e., by repressing repressor R). Error bars in *A* and *B* represent SD (n = 4 per group). (*) $P < 0.05$.

(−8.4 ± 1.9 pA/pF [n = 7] at −110 mV), while such current was virtually absent in the quiescent myocytes of *Cre4-CT* and control mice. Our experimental evidence thus showed that the ectopic expression of *TBX3* in the atria induces the formation of pacemaker activity resulting in functional ectopic nodes in the atria in vivo.

Discussion

The present study uses loss- and gain-of-function strategies and genetic lineage analysis to define the potential role of Tbx3 in the regulation of SAN formation, and identifies Tbx3 as a central regulatory factor that controls the SAN gene program and phenotype in the heart. Tbx3 appears to be sufficient to reprogram atrial cells into functional pacemaker cells. During embryonic development, Tbx3 defines the SAN region by shielding the cells within its own expression domain from atrial gene expression and differentiation, while at the same time inducing SAN gene expression. The precursor cells within this domain then expand to form the SAN, without receiving contributions from the bordering atrial myocytes, which were found to segregate soon after their differentiation. As such, these results identify a new paradigm for the specification and formation of the SAN, and provide an important aspect of the underlying molecular mechanism. *Tbx3* expression in the developing nodal components of the conduction system is conserved among higher vertebrates (Hoogaars et al. 2004), indicating that Tbx3 is an evolutionarily conserved control of SAN formation and phenotype.

Tbx3 and the formation of the SAN

Compared with the working myocardium, the cells of the SAN are small and pale and have poorly developed sarcomeres and sarcoplasmic reticulum. These nodal cells are automatic and express few gap junctions, and their intercellular coupling is poor (Bleeker et al. 1980; Canale et al. 1986). Interestingly, these properties and gene expression patterns of the SAN resemble those of the early embryonic myocytes (for review, see Moorman and Christoffels 2003). This suggests that while embryonic cardiac muscle cells differentiate and mature into working myocytes, the SAN retains properties of embryonic myocardium. We now show that *Tbx3* is expressed in the developing and mature SAN and is required to suppress the expression of atrial differentiation marker genes. These findings indicate that Tbx3 specifies the SAN domain by suppressing differentiation to working myocardium, thereby allowing the cells within its expression domain to retain the properties required for their pacemaker function in the mature heart. However, during development, the phenotype of the SAN is not fixed, but also matures. The finding that Tbx3 not only suppresses working myocardial genes, but also is required for the activity of SAN genes such as *Lbh*, and is able to induce important SAN genes including *Hcn*-family members and *Cx30.2*, indicates that Tbx3 plays an active role in the establishment of the mature SAN phenotype.

Analysis of E12.5 $Tbx3^{Cre/Cre}$ embryos revealed that a primordial SAN was formed that was variable in size. This indicates that Tbx3 may be involved in, but is not

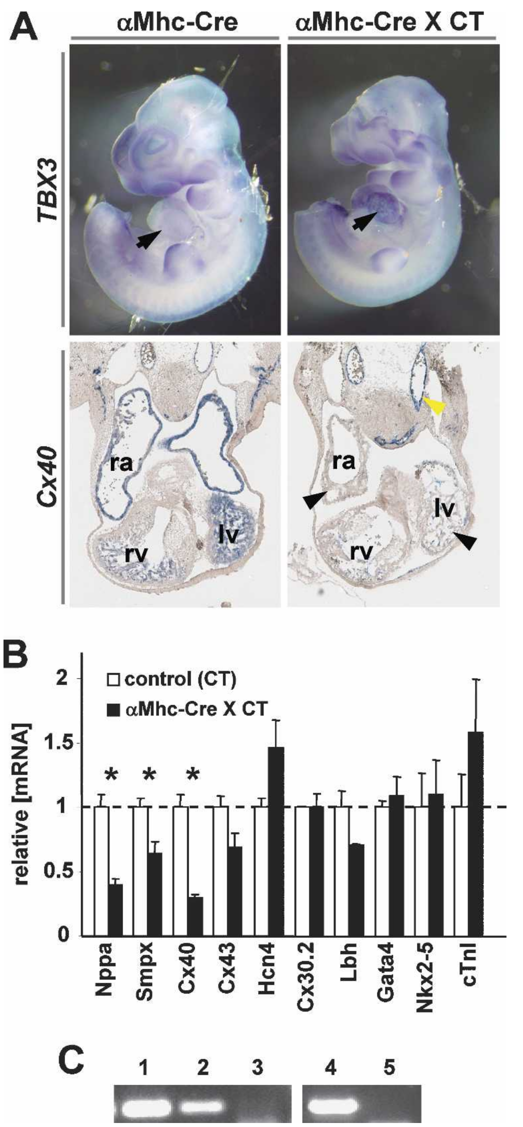

Figure 7. Activation of TBX3 in embryonic hearts leads to decreased expression of atrial genes but not up-regulation of SAN genes. (*A*) Whole-mount in situ hybridization of E10.5 α*Mhc-Cre-CT* double transgenic embryos, showing ectopic expression of *TBX3* in the whole heart (black arrow). Expression of *Cx40* is decreased specifically in the hearts of α*Mhc-Cre-CT* embryos (black arrowheads). Yellow arrow depicts staining in endothelial cells of the dorsal aorta, which is comparable in α*Mhc-Cre-CT* and α*Mhc-Cre* control embryos. (*B*) QRT–PCR analysis showed a significant down-regulation of atrium-enriched genes *Nppa*, *Smpx*, and *Cx40*, but not of SAN-enriched genes *Hcn4*, *Lbh*, and *Cx30.2*. (*C*) Chromatin was isolated from H10 rat cardiomyocyte cells stably expressing Flag-tagged Tbx3. PCR analysis of input DNA using primers surround the *Cx43* TBEs at position −450 pb is shown in lane *1*. Lane *2* and *3* show TBE target amplification using Flag-immunoprecipitated chromatin from cells expressing Flag-Tbx3 or a control not expressing Flag-Tbx3, respectively. Amplification of a region ~0.6 kb upstream of the TBE can only be achieved using the input DNA (lane *4*), whereas amplification using Flag-Tbx3-derived chromatin fails to give an amplification product (lane *5*).

strictly required for, the induction of the primordial SAN. Furthermore, the primordial SAN expressed *Cre*, indicating that Tbx3 is not required for its own expression. At E12.5 we found ectopic expression of *Cx43* and *Smpx* in the *Cre* expression domain of the primordial SAN. However, only at E13.5–E14.5 were *Cx40* and *Nppa* ectopically induced in the primordial SAN of $Tbx3^{Cre/Cre}$ embryos, suggesting redundancy of repressive Tbx3 function or the absence of an activating factor of these genes at earlier stages. The cardiac homeobox transcription factor Nkx2-5, an essential activator of *Cx40* and *Nppa* (Harvey 2002; Dupays et al. 2005), is not expressed in the SAN region until approximately E13–E14 (Mommersteeg et al. 2007), explaining why the requirement of Tbx3 to suppress *Cx40* and *Nppa* in *Tbx3*-deficient embryos only becomes apparent at this stage. Therefore, the expression of Nkx2-5-regulated genes may initially not be altered in the primordial SAN of *Tbx3*-deficient embryos.

Tbx3 is a potent transcriptional repressor (He et al. 1999). *Nppa* was shown to contain a TBE critical for the suppression of *Nppa* promoter activity in the *Tbx3*-positive atrioventricular canal in vivo, to which Tbx3 binds in vitro (Habets et al. 2002; Hoogaars et al. 2004). Also promoter fragments of *Cx40* and *Cx43* contain TBEs that are involved in T-box factor-mediated gene regulation in cell culture, and in limb in vivo (Bruneau et al. 2001; Chen et al. 2004). It is therefore likely that Tbx3 directly suppresses the activity of atrial genes in vivo. Indeed, chromatin immunoprecipitation analysis revealed that Tbx3 specifically interacts with the TBE-containing DNA region of the *Cx43* gene in HL-10 cells in vivo, providing strong indication that Tbx3 directly suppresses *Cx43*. In addition, Tbx3 was found to efficiently activate *Lbh*, previously shown to suppress the *Nppa* promoter (Briegel et al. 2005), and to suppress *Hop*, required for *Cx40* expression (Ismat et al. 2005). Therefore, we speculate that Tbx3 may suppress atrial genes both directly and indirectly through modulating the expression of suppressors and activators of atrial genes.

The repressor function of Tbx3 implies that the induction of SAN genes in the atria is indirect. Consistently, when Tbx3 was ectopically expressed in the entire heart of embryos before or during chamber differentiation using the α*Mhc-Cre* mouse line, SAN genes were not significantly induced (Fig. 7A,B), indicating that a much longer period of time is required to activate these genes, as was observed in *Cre3/4-CT* mice. Furthermore, although *Lbh* expression was lost from the SAN in *Tbx3*-deficient embryos, we did not observe loss of *Hcn4* expression, and the induction of SAN-specific genes in the atria of *Cre4-CT* mice was mosaic, again with the exception of *Lbh*, which was homogeneously induced in these atria. These observations indicate that Tbx3 does not directly induce *Hcn4* and other SAN genes, but imposes a phenotype on cells that allow those genes to be activated. To identify the underlying activation mechanism, future work will focus on the analysis of *Hcn4* and *Lbh* regulation in vivo.

Heterozygous mutations in *TBX3* causes ulnar-mam-

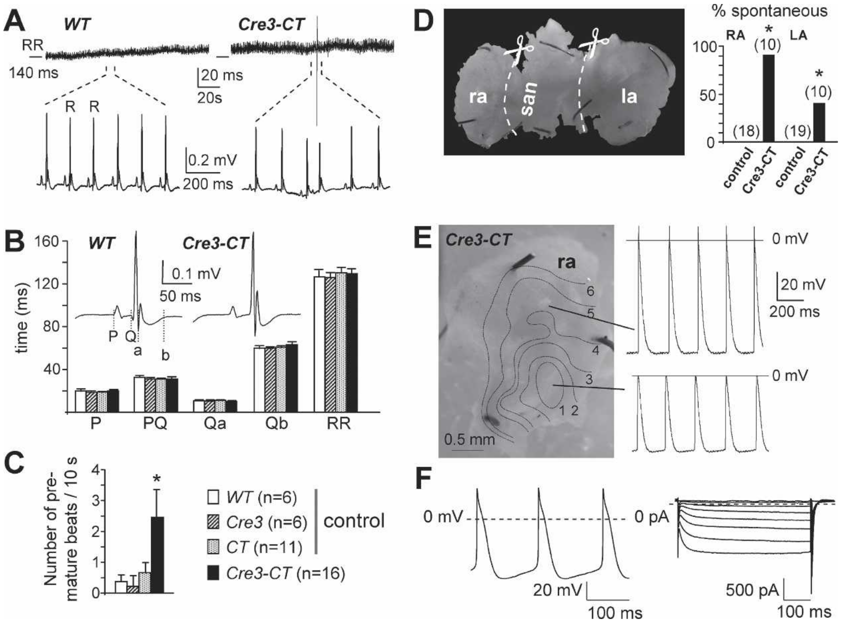

Figure 8. Ectopic pacemaker activity in *Cre3-CT* mice. (*A*) Three-minute segment of RR intervals, displaying heart rate instability. Inspection of an ECG segment in an expanded time scale revealed a premature beat in the *Cre3-CT* group. (*B*,*C*) ECG analysis uncovered an increase in premature beats in the *Cre3-CT* mice group compared with the three control groups, without changes in ECG parameters. (*D*) Only *Cre3-CT* mice showed spontaneous electrical activity in both isolated right and left atria. (*E*) Activation map of isolated right atria of *Cre3-CT* mice, showing the presence of stable ectopic nodal impulse formation originating from the site marked by an asterisk. The numbers on isochrones indicate activation time in milliseconds. (*F*) Typical example of pacemaker formation (*left*) and hyperpolarization-activated current (*right*) in a single right atrial *Cre4-CT* cardiomyocyte. (*) $P < 0.05$.

mary syndrome in human, but mice appear to be less sensitive to a lower Tbx3 dose (Naiche et al. 2005). Consistently, we did not observe alterations in gene expression in the SAN of heterozygous $Tbx3^{+/-}$ embryos and adults. Affected conduction system morphology or function has not been reported in ulnar-mammary syndrome patients, suggesting that the reduced *TBX3* dose is sufficient for SAN regulation in humans. However, a subset of ulnar-mammary syndrome patients has structural congenital heart defects, indicating that reduction of Tbx3 dose in the context of certain genetic backgrounds or additional mutations becomes important for heart development. It is therefore possible that a closer examination of a large number of ulnar-mammary syndrome patients may reveal conduction system anomalies.

Formation of the SAN: recruitment versus proliferation of specified precursors

The central conduction system components have been proposed to form by continuous recruitment throughout development of myocytes into an initial framework of specified conduction system cells. This proposal was based on elegant retrospective clonal analyses in which rare single-cell-derived clones found in the central conduction system always extended into the adjacent working myocardium (Cheng et al. 1999; Pennisi et al. 2002). The phenotype of the infected founder cell could not be assessed. However, during development, the cells of the central conduction system, including those of the SAN (Erokhina and Rumyantsev 1986), proliferate much less compared with the adjacent myocytes forming the working myocardium, which indicated that the latter enter the conduction system lineage, rather than the other way around (Cheng et al. 1999). The spatio-temporal expression patterns we observed indicate specification of the sinoatrial junction in *Tbx3*/*Hcn4*-positive nodal precursors and adjacent *Cx40*/*Nppa*-positive atrial precursors as early as E10. Therefore, SAN specification and growth can be envisioned to follow either of two modes as presented in Figure 3, A and B. Using the Cre-loxP system, the emerging atrial lineage bordering the *Tbx3*-positive domain was irreversibly labeled, allowing assessment of recruitment of the atrial cells into the SAN lineage. We found that the pattern of β-galactosidase or EGFP, irreversibly activated by the *Nppa-Cre* allele from E10 on, exactly matched the patterns of *Cx40* and *Nppa* expression and was strictly complementary to those of *Tbx3* and *Hcn4* expression. These data indicate that from their differentiation onward, atrial myocytes are not recruited into the SAN lineage. Our assay did not rule out the possibility that initially *Tbx3*-positive cells differentiate to atrial working myocardium later in development. *Tbx3* expression was observed to be associated with the SAN during development. In addition, Tbx3 was found to be able to suppress the atrial genes, including the *Nppa-Cre* cassette used to label atrial myocytes, and appeared to be required to suppress atrial genes in the primordial SAN. From the combined data, we conclude that the mature SAN is formed from the *Tbx3*-positive embryonic precursor population.

Tbx3 imposes pacemaker activity on atrial myocytes

Many time-dependent currents contribute to SAN function. These currents are encoded by several gene families, each comprising several family members (Boyett et al. 2000; Schram et al. 2002; Marionneau et al. 2005). Other important properties include intercellular coupling, which is largely defined by the number and type of gap junctions present in and around the SAN. The difference in function between atrial working myocytes and SAN cells is at least in part defined by genes differentially expressed between the SAN and atria. To date, only a limited number of differentially expressed genes have been identified, but their contribution to either SAN-specific or atrial working myocardial-specific function is substantial. Some of these genes were found to be essential for pacemaker function or for impulse propagation, whereas others are sufficient to generate ectopic pacemaker activity (Miake et al. 2002; Papadatos et al. 2002; Schram et al. 2002; Rosen et al. 2004; Stieber et al. 2004; Bucchi et al. 2006; Tse et al. 2006). In the present study, we found the remarkable ability of Tbx3 to selectively regulate the expression of this differentially expressed and functionally important set of genes, indicating that it acts upstream in a pathway that controls pacemaker phenotype. Not only does it repress genes required for working myocardial function, it also stimulates genes required for pacemaker function, including pacemaker channels (Hcn), calcium channel (Cav3.1), and slow gap junction Cx30.2, thereby efficiently reprogramming atrial myocytes into functional pacemaker cells. In contrast, genes not implicated in the functional or structural distinction between atria and SAN were not affected by Tbx3. These results indicate that Tbx3 is an efficient tool to identify genes that define the distinction between working myocardium and pacemaker cells, and to gain further insight into the molecular genetic underpinnings of pacemaker formation and function.

Currently, attempts to generate bio-artificial pacemakers with normal entopic electrophysiological characteristics using virally delivered channel genes are ongoing (Miake et al. 2002; Rosen et al. 2004; Bucchi et al. 2006; Tse et al. 2006). These pacemakers provide a novel inroad into treatment of common arrhythmias. It will be of great clinical interest to examine whether Tbx3 could be applied in the generation of bio-artificial pacemakers. Although Tbx3 maintains proliferation and stimulates senescence bypass in specific cell types (Brummelkamp et al. 2002; Naiche et al. 2005), it is unlikely to have this role in developing or mature cardiac myocytes, possibly rendering it a useful tool to reprogram working myocytes ex vivo into pacemaker cells displaying normal electrophysiological characteristics.

Materials and methods

Mice and gene targeting

Z/EG (Novak et al. 2000) and *R26R* (Soriano 1999) reporter mice have been described previously. The *CAG–CAT–TBX3* (*CT*) transgene construct harbors a human *TBX3* cDNA encoding a full-length human TBX3 protein (Brummelkamp et al. 2002) with an in-frame fusion to a hemagglutinin (HA) tag in a modified backbone from *pCAG–CAT–Z* (Araki et al. 1995). *CT* transgenic mice were bred with *Nppa-Cre3*, *Nppa-Cre4* (de Lange et al. 2003), or *αMhc-Cre* mice (Agah et al. 1997) to generate double-transgenic mice conditionally expressing *TBX3* in the atria or the whole heart, respectively. The transgenic mice were identified by PCR analysis using primers specific for *CAT* and *Cre* genes.

A cosmid with *Tbx3*, isolated from the 129/Ola cosmid genomic library obtained from the Resourcenzentrum (RZPD) in Berlin, was kindly provided by Dr. Andreas Kispert (Institut fur Molekularbiologie, Medizinische Hochschule Hannover, Hannover, Germany). Homologous DNA sequences (6.1 kb of upstream sequence and 1.9 kb of downstream sequence) were ligated to a Cre-polyA-Frt-flanked PGK-neo cassette derived from pKOII (Bardeesy et al. 2002) to generate a *Tbx3*-targeting construct (Supplementary Fig. 2) in which the first three codons of the *Tbx3*-coding region were replaced by the *Cre-pA* cassette. The linearized targeting construct was electroporated into E141B10 embryonic stem (ES) cells to generate targeted cell lines. A diphtheria toxin A cassette was used to positively select for homologous recombinants. Chimeras were generated by injection of targeted ES cells into C57Bl6 host blastocysts. Germline transmission of the targeted allele was obtained by mating with FVB females. Subsequently, $Tbx3^{CreNEO}$ mice were crossed with FlpE mice (Rodriguez et al. 2000) to remove the PGK-neo cassette. Progeny was screened by PCR for the presence of the $Tbx3^{Cre}$ allele using the following primers: fw1 (AGCGGAGCCAAGCCAGCA), rv1 (CCTTGGCCTCCAG GTGCAC), and rv2 (GCTAGAGCCTGTTTTGCACGTTCA). The $Tbx3^{Cre}$ allele has been maintained on a FVB background. Animal care was in accordance with national and institutional guidelines.

Chromatin immunoprecipitation

Chromatin was isolated from the rat neonatal cardiomyocyte cell line, H10 (Jahn et al. 1996), stably expressing Flag-tagged Tbx3. A kit (Active Motif) and Flag M2 Sepharose (Sigma) were used to capture the Flag-tagged protein according to the manufacturer's instructions. DNA fragments were analyzed by PCR with primers specific for the rat *Cx43* TBEs ~450 base pairs (bp) upstream of the transcription start site (5′-CCGTGTTTAAGA GGAGGAGAATTAGG-3′ and 5′-GGGACAAGGTCAACTCG TGCAGAC-3′) or for the control region ~1 kb upstream (5′-AG GAGCTGCCCACCCTTAGGAATG-3′ and 5′-GAGTTTCCA GATACATTATGTTAGC-3′).

In situ hybridization, immunohistochemistry, and histology

Nonradioactive in situ hybridization, 3D reconstruction, and quantification of expression domains were performed as described previously (Moorman et al. 2001; Hoogaars et al. 2004). The probes used have been described previously (Hoogaars et al. 2004). Probes for *Hcn4* (Santoro et al. 2000; Garcia-Frigola et al. 2003) and *Hop* (Chen et al. 2002) were generously provided by B. Santoro (Center for Neurobiology and Behavior, Columbia University, New York, NY) and J. Epstein (Department of Cell and Developmental Biology, University of Pennsylvania School of Medicine, Philadelphia, PA), respectively. For immunohistochemistry, adult hearts were isolated in PBS, rapidly frozen in liquid nitrogen, and cut into 10-µm sections. The primary antibodies used were HCN4 rabbit polyclonal (1:250; Chemicon), Cx40 rabbit polyclonal (1:250; Chemicon), Cx43 mouse monoclonal (1:250; BD Transduction Laboratory), cTnI rabbit polyclonal (1:1000; Hitest Ltd.), and Nav1.5 rabbit polyclonal (1:100; Alomone Laboratories). The secondary antibodies used were Alexa 647 anti-rabbit, Alexa 568 anti-rabbit, and Alexa 568 anti-mouse antibodies (1:100; Molecular Probes). Nuclei were stained using Sytox Green nucleic acid stain (1:30,000; Molecular Probes). Fibrosis was determined by Pico Sirius red staining.

Quantitative expression analysis

Total RNA was isolated from atrial appendices of adult mice (2–4 mo) using the RNeasy Mini Kit according to the manufacturer's protocol (Qiagen). cDNA was reverse-transcribed from 300 ng of total RNA using the SuperScript II system (Invitrogen). Expression of different genes was assayed with quantitative real-time PCR using the MyiQ Single-Color RT–PCR Detection System (Bio-Rad). The relative start concentration [$N_{(0)}$] was calculated using the following equation: $N^{(0)} = 10^{[\log(\text{threshold})-\text{Ct}(\text{mean Eff})]}$. Values were normalized to *Gapdh* expression levels.

ECGs

Lead I ECG configuration recordings were obtained in anesthetized (isofluraan 1.5%) mice. Plots of successive RR intervals during 15-min epochs were inspected for periods of irregularity in heart rate. Premature beats were defined as a rhythm during which P waves occurred prior to the expected P wave.

Electrophysiology

Electrophysiological mapping of the atrial region was accomplished at 37.0 ± 0.3°C as recently described (Verheijck et al. 2001). Transmembrane potentials were recorded at 5 kHz by conventional glass microelectrodes filled with 2.7 M KCl and 2 mM K-citrate (resistance 15–30 MΩ). For the construction of activation maps, impalements were made 0.1 mm apart and in the ectopic pacemaker area down to 0.05 mm apart. Ectopic pacemakers showed diastolic depolarization and low maximal upstroke velocity <10 V/sec. A bipolar silver wire electrode was placed on the edge of the preparation. This electrode provided a surface electrogram of which the first deflection served as a time reference for the determination of the ectopic conduction time and construction of the activation map. Single right atrial cardiomyocytes were isolated by enzymatic dissociation. Action potentials and hyperpolarizing-activated currents were recorded using the perforated patch-clamp technique (Axopatch 200B Clamp amplifier; Axon Instruments, Inc.). Signals were low-pass-filtered (cut-off frequency 5 kHz) and digitized at 5 kHz. Series resistance was compensated ≥80%, and potentials were corrected for liquid-junction potential. For voltage control, data acquisition, and analysis, custom-made software was used. The superfusion solution (37°C) contained 140 mM NaCl, 5.4 mM KCl, 1.8 mM $CaCl_2$, 1 mM $MgCl_2$, 5.5 mM glucose, and 5 mM HEPES [pH 7.4 (NaOH)]. The pipette solution contained 125 mM K-gluc, 20 mM KCl, 5 mM NaCl, 2.2 mM amphotericin-B, and 10 mM HEPES [pH 7.2 (KOH)]. Hyperpolarizing-activated current was measured by 500-msec hyperpolarizing steps from −40 mV.

Statistics

Results are expressed as mean ± SEM. Data are considered different if $P < 0.05$. The Mann-Whitney U-test, unpaired *t*-test, or Fisher's exact test was used if appropriate.

Acknowledgments

We thank Tilly Mommersteeg, Kees Jan Boogerd, Jan Ruijter, André Linnenbank, Corrie de Gier-de Vries, Alexandre Soufan, Ephie Kraneveld, and Toon van Veen for their contributions and advice; the GGM facility for generating mice; Susan Dymecki for providing *FlpE* deleter mice; Michael Schneider for providing *αMhc-Cre* mice; and Andreas Kispert, Bina Santoro, Ronald DePinho, Jonathan Epstein, and Jun-ichi Miyazaki for reagents. This work was supported by NWO 912-03-043 to E.E.V. and V.M.C.; by NHS grant 1996M002 to A.F.M. and V.M.C.; by NWO 864-05-006 to V.M.C.; and by NHS grant 2005B076 to V.M.C.

References

Agah, R., Frenkel, P.A., French, B.A., Michael, L.A., Overbeek, P.A., and Schneider, M.D. 1997. Gene recombination in postmitotic cells. Targeted expression of Cre recombinase provokes cardiac-restricted, site-specific rearrangement in adult ventricular muscle in vivo. *J. Clin. Invest.* **100:** 169–179.

Araki, K., Araki, M., Miyazaki, J., and Vassalli, P. 1995. Site-specific recombination of a transgene in fertilized eggs by transient expression of Cre recombinase. *Proc. Natl. Acad. Sci.* **92:** 160–164.

Bagwe, S., Berenfeld, O., Vaidya, D., Morley, G.E., and Jalife, J. 2005. Altered right atrial excitation and propagation in connexin40 knockout mice. *Circulation* **112:** 2245–2253.

Bamshad, M., Lin, R.C., Law, D.J., Watkins, W.C., Krakowiak, P.A., Moore, M.E., Franceschini, P., Lala, R., Holmes, L.B., Gebuhr, T.C., et al. 1997. Mutations in human TBX3 alter limb, apocrine and genital development in ulnar-mammary syndrome. *Nat. Genet.* **16:** 311–315.

Bardeesy, N., Sinha, M., Hezel, A.F., Signoretti, S., Hathaway, N.A., Sharpless, N.E., Loda, M., Carrasco, D.R., and DePinho, R.A. 2002. Loss of the Lkb1 tumour suppressor provokes intestinal polyposis but resistance to transformation. *Nature* **419:** 162–167.

Baruscotti, M., Bucchi, A., and DiFrancesco, D. 2005. Physiology and pharmacology of the cardiac pacemaker ('funny') current. *Pharmacol. Ther.* **107:** 59–79.

Bleeker, W.K., Mackaay, A.J.C., Masson-Pevet, M., Bouman, L.N., and Becker, A.E. 1980. Functional and morphological organization of the rabbit sinus node. *Circ. Res.* **46:** 11–22.

Boyett, M.R., Honjo, H., and Kodama, I. 2000. The sinoatrial node, a heterogeneous pacemaker structure. *Cardiovasc. Res.* **47:** 658–687.

Briegel, K.J., Baldwin, H.S., Epstein, J.A., and Joyner, A.L. 2005. Congenital heart disease reminiscent of partial trisomy 2p syndrome in mice transgenic for the transcription factor Lbh. *Development* **132:** 3305–3316.

Brummelkamp, T.R., Kortlever, R.M., Lingbeek, M., Trettel, F., MacDonald, M.E., van Lohuizen, M., and Bernards, R. 2002. TBX-3, the gene mutated in Ulnar-Mammary Syndrome, is a negative regulator of p19ARF and inhibits senescence. *J. Biol. Chem.* **277:** 6567–6572.

Bruneau, B.G., Nemer, G., Schmitt, J.P., Charron, F., Robitaille, L., Caron, S., Conner, D.A., Gessler, M., Nemer, M., Seidman, C.E., et al. 2001. A murine model of Holt-Oram syndrome defines roles of the T-box transcription factor Tbx5 in cardiogenesis and disease. *Cell* **106:** 709–721.

Bucchi, A., Plotnikov, A.N., Shlapakova, I., Danilo Jr., P., Kryukova, Y., Qu, J., Lu, Z., Liu, H., Pan, Z., Potapova, I., et al. 2006. Wild-type and mutant HCN channels in a tandem biological-electronic cardiac pacemaker. *Circulation* **114:** 992–999.

Canale, E.D., Campbell, G.R., Smolich, J.J., and Campbell, J.H. 1986. *Cardiac muscle.* Springer Verlag, Berlin.

Carlson, H., Ota, S., Song, Y., Chen, Y., and Hurlin, P.J. 2002. Tbx3 impinges on the p53 pathway to suppress apoptosis, facilitate cell transformation and block myogenic differentiation. *Oncogene* **21:** 3827–3835.

Chen, F., Kook, H., Milewski, R., Gitler, A.D., Lu, M.M., Li, J., Nazarian, R., Schnepp, R., Jen, K., Biben, C., et al. 2002. Hop is an unusual homeobox gene that modulates cardiac development. *Cell* **110:** 713–723.

Chen, J.R., Chatterjee, B., Meyer, R., Yu, J.C., Borke, J.L., Isales, C.M., Kirby, M.L., Lo, C.W., and Bollag, R.J. 2004. Tbx2 represses expression of connexin43 in osteoblastic-like cells.

Calcif. Tissue Int. **74:** 561–573.

Cheng, G., Litchenberg, W.H., Cole, G.J., Mikawa, T., Thompson, R.P., and Gourdie, R.G. 1999. Development of the cardiac conduction system involves recruitment within a multipotent cardiomyogenic lineage. *Development* **126:** 5041–5049.

Christoffels, V.M., Habets, P.E.M.H., Franco, D., Campione, M., de Jong, F., Lamers, W.H., Bao, Z.Z., Palmer, S., Biben, C., Harvey, R.P., et al. 2000. Chamber formation and morphogenesis in the developing mammalian heart. *Dev. Biol.* **223:** 266–278.

Christoffels, V.M., Burch, J.B.E., and Moorman, A.F.M. 2004a. Architectural plan for the heart: Early patterning and delineation of the chambers and the nodes. *Trends Cardiovasc. Med.* **14:** 301–307.

Christoffels, V.M., Hoogaars, W.M.H., Tessari, A., Clout, D.E.W., Moorman, A.F.M., and Campione, M. 2004b. T-box transcription factor Tbx2 represses differentiation and formation of the cardiac chambers. *Dev. Dyn.* **229:** 763–770.

Davenport, T.G., Jerome-Majewska, L.A., and Papaioannou, V.E. 2003. Mammary gland, limb and yolk sac defects in mice lacking Tbx3, the gene mutated in human ulnar mammary syndrome. *Development* **130:** 2263–2273.

de Lange, F.J., Moorman, A.F.M., and Christoffels, V.M. 2003. Atrial cardiomyocyte-specific expression of Cre recombinase driven by an Nppa gene fragment. *Genesis* **37:** 1–4.

Dupays, L., Jarry-Guichard, T., Mazurais, D., Calmels, T., Izumo, S., Gros, D., and Theveniau-Ruissy, M. 2005. Dysregulation of connexins and inactivation of NFATc1 in the cardiovascular system of Nkx2-5 null mutants. *J. Mol. Cell. Cardiol.* **38:** 787–798.

Erokhina, I.L. and Rumyantsev, P.P. 1986. Ultrastructure of DNA-synthesizing and mitotically dividing myocytes in sinoatrial node of mouse embryonal heart. *J. Mol. Cell. Cardiol.* **18:** 1219–1231.

Garcia-Frigola, C., Shi, Y., and Evans, S.M. 2003. Expression of the hyperpolarization-activated cyclic nucleotide-gated cation channel HCN4 during mouse heart development. *Brain Res. Gene Expr. Patterns* **3:** 777–783.

Gros, D., Dupays, L., Alcolea, S., Meysen, S., Miquerol, L., and Theveniau-Ruissy, M. 2004. Genetically modified mice: Tools to decode the functions of connexins in the heart—New models for cardiovascular research. *Cardiovasc. Res.* **62:** 299–308.

Habets, P.E.M.H., Moorman, A.F.M., Clout, D.E.W., van Roon, M.A., Lingbeek, M., Lohuizen, M., and Christoffels, V.M. 2002. Cooperative action of Tbx2 and Nkx2.5 inhibits ANF expression in the atrioventricular canal: Implications for cardiac chamber formation. *Genes & Dev.* **16:** 1234–1246.

Harrelson, Z., Kelly, R.G., Goldin, S.N., Gibson-Brown, J.J., Bollag, R.J., Silver, L.M., and Papaioannou, V.E. 2004. Tbx2 is essential for patterning the atrioventricular canal and for morphogenesis of the outflow tract during heart development. *Development* **131:** 5041–5052.

Harvey, R.P. 2002. Patterning the vertebrate heart. *Nat. Rev. Genet.* **3:** 544–556.

He, M., Wen, L., Campbell, C.E., Wu, J.Y., and Rao, Y. 1999. Transcription repression by *Xenopus* ET and its human ortholog TBX3, a gene involved in ulnar-mammary syndrome. *Proc. Natl. Acad. Sci.* **96:** 10212–10217.

Hoogaars, W.M.H., Tessari, A., Moorman, A.F.M., de Boer, P.A.J., Hagoort, J., Soufan, A.T., Campione, M., and Christoffels, V.M. 2004. The transcriptional repressor Tbx3 delineates the developing central conduction system of the heart. *Cardiovasc. Res.* **62:** 489–499.

Ismat, F.A., Zhang, M., Kook, H., Huang, B., Zhou, R., Ferrari, V.A., Epstein, J.A., and Patel, V.V. 2005. Homeobox protein Hop functions in the adult cardiac conduction system. *Circ. Res.* **96:** 898–903.

Jahn, L., Sadoshima, J., Greene, A., Parker, C., Morgan, K.G., and Izumo, S. 1996. Conditional differentiation of heart- and smooth muscle-derived cells transformed by a temperature-sensitive mutant of SV40 T antigen. *J. Cell Sci.* **109:** 397–407.

Keith, A. and Flack, M. 1907. The form and nature of the muscular connections between the primary divisions of the vertebrate heart. *J. Anat. Physiol.* **41:** 172–189.

Kreuzberg, M.M., Schrickel, J.W., Ghanem, A., Kim, J.S., Degen, J., Janssen-Bienhold, U., Lewalter, T., Tiemann, K., and Willecke, K. 2006. Connexin30.2 containing gap junction channels decelerate impulse propagation through the atrioventricular node. *Proc. Natl. Acad. Sci.* **103:** 5959–5964.

Lei, M., Jones, S.A., Liu, J., Lancaster, M.K., Fung, S.S.M., Dobrzynski, H., Camelliti, P., Maier, S.K.G., Noble, D., and Boyett, M.R. 2004. Requirement of neuronal- and cardiac-type sodium channels for murine sinoatrial node pacemaking. *J. Physiol.* **559:** 835–848.

Liu, J., Dobrzynski, H., Yanni, J., Boyett, M.R., and Lei, M. 2006. Organisation of the mouse sinoatrial node: Structure and expression of HCN channels. *Cardiovasc. Res.* **73:** 729–738.

Mangoni, M.E., Traboulsie, A., Leoni, A.L., Couette, B., Marger, L., Le, Q.K., Kupfer, E., Cohen-Solal, A., Vilar, J., Shin, H.S., et al. 2006. Bradycardia and slowing of the atrioventricular conduction in mice lacking Cav3.1/α1G T-type calcium channels. *Circ. Res.* **98:** 1422–1430.

Marionneau, C., Couette, B., Liu, J., Li, H., Mangoni, M.E., Nargeot, J., Lei, M., Escande, D., and Demolombe, S. 2005. Specific pattern of ionic channel gene expression associated with pacemaker activity in the mouse heart. *J. Physiol.* **562:** 223–234.

Meneghini, V., Odent, S., Platonova, N., Egeo, A., and Merlo, G.R. 2006. Novel TBX3 mutation data in families with Ulnar-Mammary syndrome indicate a genotype–phenotype relationship: Mutations that do not disrupt the T-domain are associated with less severe limb defects. *Eur. J. Med. Genet.* **49:** 151–158.

Miake, J., Marban, E., and Nuss, H.B. 2002. Biological pacemaker created by gene transfer. *Nature* **419:** 132–133.

Milanesi, R., Baruscotti, M., Gnecchi-Ruscone, T., and DiFrancesco, D. 2006. Familial sinus bradycardia associated with a mutation in the cardiac pacemaker channel. *N. Engl. J. Med.* **354:** 151–157.

Mommersteeg, M.T., Hoogaars, W.M., Prall, O.W., de Gier-de Vries, C., Wiese, C., Clout, D.E., Papaioannou, V.E., Brown, N.A., Harvey, R.P., Moorman, A.F., et al. 2007. Molecular pathway for the localized formation of the sinoatrial node. *Circ. Res.* **100:** 354–362.

Moorman, A.F.M. and Christoffels, V.M. 2003. Cardiac chamber formation: Development, genes and evolution. *Physiol. Rev.* **83:** 1223–1267.

Moorman, A.F.M., Houweling, A.C., de Boer, P.A.J., and Christoffels, V.M. 2001. Sensitive non-radioactive detection of mRNA in tissue sections: Novel application of the whole-mount in situ hybridization protocol. *J. Histochem. Cytochem.* **49:** 1–8.

Naiche, L.A., Harrelson, Z., Kelly, R.G., and Papaioannou, V.E. 2005. T-Box genes in vertebrate development. *Annu. Rev. Genet.* **39:** 219–239.

Novak, A., Guo, C., Yang, W., Nagy, A., and Lobe, C.G. 2000. Z/EG, a double reporter mouse line that expresses enhanced green fluorescent protein upon Cre-mediated excision. *Genesis* **28:** 147–155.

Papadatos, G.A., Wallerstein, P.M., Head, C.E., Ratcliff, R., Brady, P.A., Benndorf, K., Saumarez, R.C., Trezise, A.E., Huang, C.L., Vandenberg, J.I., et al. 2002. Slowed conduction and ventricular tachycardia after targeted disruption of the cardiac sodium channel gene Scn5a. *Proc. Natl. Acad. Sci.* **99:** 6210–6215.

Pennisi, D.J., Rentschler, S., Gourdie, R.G., Fishman, G.I., and Mikawa, T. 2002. Induction and patterning of the cardiac conduction system. *Int. J. Dev. Biol.* **46:** 765–775.

Rodriguez, C.I., Buchholz, F., Galloway, J., Sequerra, R., Kasper, J., Ayala, R., Stewart, A.F., and Dymecki, S.M. 2000. High-efficiency deleter mice show that FLPe is an alternative to Cre-loxP. *Nat. Genet.* **25:** 139–140.

Rosen, M.R., Brink, P.R., Cohen, I.S., and Robinson, R.B. 2004. Genes, stem cells and biological pacemakers. *Cardiovasc. Res.* **64:** 12–23.

Santoro, B., Chen, S., Luthi, A., Pavlidis, P., Shumyatsky, G.P., Tibbs, G.R., and Siegelbaum, S.A. 2000. Molecular and functional heterogeneity of hyperpolarization-activated pacemaker channels in the mouse CNS. *J. Neurosci.* **20:** 5264–5275.

Schram, G., Pourrier, M., Melnyk, P., and Nattel, S. 2002. Differential distribution of cardiac ion channel expression as a basis for regional specialization in electrical function. *Circ. Res.* **90:** 939–950.

Schulze-Bahr, E., Neu, A., Friederich, P., Kaupp, U.B., Breithardt, G., Pongs, O., and Isbrandt, D. 2003. Pacemaker channel dysfunction in a patient with sinus node disease. *J. Clin. Invest.* **111:** 1537–1545.

Soriano, P. 1999. Generalized lacZ expression with the ROSA26 Cre reporter strain. *Nat. Genet.* **21:** 70–71.

Stieber, J., Herrmann, S., Feil, S., Loster, J., Feil, R., Biel, M., Hofmann, F., and Ludwig, A. 2003. The hyperpolarization-activated channel HCN4 is required for the generation of pacemaker action potentials in the embryonic heart. *Proc. Natl. Acad. Sci.* **100:** 15235–15240.

Stieber, J., Hofmann, F., and Ludwig, A. 2004. Pacemaker channels and sinus node arrhythmia. *Trends Cardiovasc. Med.* **14:** 23–28.

Tse, H.F., Xue, T., Lau, C.P., Siu, C.W., Wang, K., Zhang, Q.Y., Tomaselli, G.F., Akar, F.G., and Li, R.A. 2006. Bioartificial sinus node constructed via in vivo gene transfer of an engineered pacemaker HCN channel reduces the dependence on electronic pacemaker in a sick-sinus syndrome model. *Circulation* **114:** 1000–1011.

Verheijck, E.E., van Kempen, M.J., Veereschild, M., Lurvink, J., Jongsma, H.J., and Bouman, L.N. 2001. Electrophysiological features of the mouse sinoatrial node in relation to connexin distribution. *Cardiovasc. Res.* **52:** 40–50.

Yamamoto, M., Dobrzynski, H., Tellez, J., Niwa, R., Billeter, R., Honjo, H., Kodama, I., and Boyett, M.R. 2006. Extended atrial conduction system characterised by the expression of the HCN4 channel and connexin45. *Cardiovasc. Res.* **72:** 271–281.